Construction of coronal models for H2 d3Πu–a3Σg+ and I1Πg–B1Σu+ transitions for the evaluation of ro-vibrational temperatures

AUTHOR(S):

Shikama, T.; Kado, S.; Iida, Y.; Suzuki, K.

Construction of coronal models for H_2 $d^3\Pi_u$-$a^3\Sigma_g^+$ and $I^1\Pi_g$-$B^1\Sigma_u^+$ transitions for the evaluation of ro-vibrational temperatures

T. Shikama[a*], S. Kado[b], Y. Iida[b], and K. Suzuki[b]

[a]Department of Mechanical Engineering and Science,
Graduate School of Engineering, Kyoto University, Kyoto 606-8501, Japan

[b]Department of Nuclear Engineering and Management,
School of Engineering, the University of Tokyo, Tokyo 113-8656, Japan

Excitation-emission models for the H_2 $d^3\Pi_u$-$a^3\Sigma_g^+$ and $I^1\Pi_g$-$B^1\Sigma_u^+$ transitions have been developed based on the coronal approximation. The ground state ro-vibrational temperatures evaluated from the I-B transition are significantly higher than those from the d-a transition. The results may suggest the violation of the coronal approximation for the I-B transition.

1. Introduction

Ro-vibrationally excited hydrogen molecules are of interest for their contributions to the enhancement of the plasma recombination, production of the negative ions, and their utility in deducing the gas temperature. In order to obtain the state resolved ro-vibrational population densities, several techniques have been developed up to now [1–6]. Among them, optical emission spectroscopy has been widely applied for its easily applicability. However, since diatomic molecules have no permanent electric dipole moments, the measurement of the electronic ground state can only be achieved indirectly by evaluating the excitation and de-excitation processes related to the excited states [4–6]. Moreover, the most electronic excited states of hydrogen molecules are known to have perturbations, and these states cannot be analyzed by means of the adiabatic approximation. The remaining states described within the adiabatic approximation are therefore important.

In the visible wavelength region, the $d^3\Pi_u^-$-$a^3\Sigma_g^+$ transition[2], known as the Fulcher-α Q-branch, has been widely used. With the aid of well-established datasets for the excitation-emission processes, coronal models were developed [5–7]. Among the other transitions, the $I^1\Pi_g$-$B^1\Sigma_u^+$ transition lying in around 380-600 nm region has relatively large emission intensity. It may be possible to treat one of the upper states $I^1\Pi_g^-$ by the adiabatic theory without large error [8].

In this paper, we models excitation and emission processes concerning the d-a and I-B transitions based on the coronal approximation. We compare the ro-vibrational temperatures of the electronic ground state obtained from both the transitions in a low-temperature glow discharge plasma, and evaluate the validity of the coronal approximation in determining these temperatures.

2. Coronal model

The ro-vibrational temperatures in the electronic excited states of hydrogen molecules are not usually in the thermal equilibrium with those in the ground state, and the excitation-emission modeling provides an association between the temperatures in both the states. In the coronal equilibrium, the electron-impact excitation from

*e-mail: shikama@me.kyoto-u.ac.jp

[2]Here we use conventional notations $\Pi^{\pm}$. $\Pi^{\pm}$ indicate the states having the rotational wave functions $|\phi_r\rangle = (|\eta\Lambda\rangle \pm |\eta - \Lambda\rangle)/\sqrt{2}$, respectively, where Λ is the projection of the angular momentum $\boldsymbol{N}$ onto the internuclear axis and η is the remaining quantum numbers not explicitly written.

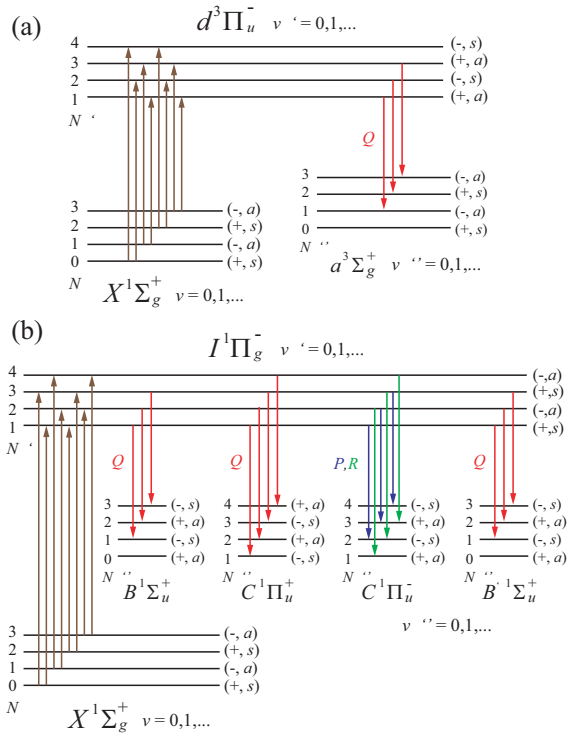

Figure 1. Schematic diagrams of the coronal equilibrium among the (a) $X^1\Sigma_g^+$, $a^3\Sigma_g^+$, and $d^3\Pi_u^-$, and (b) $X^1\Sigma_g^+$, $B^1\Sigma_u^+$, $C^1\Pi_u$, $B'^1\Sigma_u^+$, and $I^1\Pi_g^-$ states.

the ground state ($X^1\Sigma_g^+$) to the upper state (d or I) balances the radiative de-excitation from the upper state to the lower states (a or B, $C^1\Pi_u$, and $B'^1\Sigma_u^+$) as shown in Fig. 1, where we have neglected the $D^1\Pi_u$ state because of the small transition probability. In the figure, $+/-$ denotes the parity with respect to the space inversion, and s/a denotes the symmetry and asymmetry with respect to the permutation of nuclei.

The population density in the upper state with the vibrational quantum number v and rotational quantum number N is experimentally obtained from the ro-vibronic transition intensity, which is expressed using Hund's case (b) notation as

$$I_{v''N''}^{v'N'} = n_{v'N'} \frac{16\pi^3}{3\epsilon_0 c^3} \nu_{v''N''}^{v'N'\ 4} \frac{|\langle\phi'|\mu_e|\phi''\rangle|^2}{2N'+1}, \tag{1}$$

where variables with prime and double prime denote the upper and lower states, respectively, $n_{v'N'}$ is the upper state population density, ϵ_0 is the vacuum permittivity, c is the velocity of light, $\nu_{v''N''}^{v'N'}$ is the transition frequency, μ_e is the transition electric dipole moment, and $|\phi\rangle = |\phi_e\rangle|\phi_v\rangle|\phi_r\rangle$ is the total wave function divided into the electronic (e), vibrational (v), and rotational (r) wave functions. For hydrogen molecules, the electric dipole moment is not a weak function of the internuclear distance [6, 9, 10], then the line strength can be approximated as $|\langle\phi'|\mu_e|\phi''\rangle|^2 = P_{v''N''}^{v'N'} S_{N''}^{N'}$, where $P_{v''N''}^{v'N'} = |\langle\phi_v'|\langle\phi_e'|\mu_e|\phi_e''\rangle|\phi_v''\rangle|^2$ is the vibronic transition probability, and $S_{N''}^{N'}$ is the Hönl-London factor.

In the coronal approximation, the upper state population $n_{v'N'}$ is described as

$$n_{v'N'} = \frac{n_e \sum_{v,N} \left[n_{vN} \langle\sigma_e v_e\rangle_{v'N'}^{vN} \right]}{\sum_{v''N''} A_{v''N''}^{v'N'}}, \tag{2}$$

where variables not marked with prime denote the X-state, n_e is the electron density, and $A_{v''N''}^{v'N'}$ is the spontaneous emission coefficient. In the denominator, the summation is performed for several electronic states. We assume the Boltzmann ro-vibrational population distribution [11] in the X-state as

$$n_{vN} = n_{v=0} \exp\left[-\frac{\Delta G(v)}{kT_{vib}}\right] \times \frac{g_{as}(2N+1)\exp\left[-\frac{\Delta F(N,v)}{kT_{rot}}\right]}{\sum_N g_{as}(2N+1)\exp\left[-\frac{\Delta F(N,v)}{kT_{rot}}\right]}, \tag{3}$$

where $n_{v=0}$ is the population in the vibrational ground state, g_{as} is the nuclear-spin statistical weight, $\Delta G(v)$ and $\Delta F(N,v)$ are the vibrational and rotational energies from their ground states, respectively, and T_{vib} and T_{rot} are the vibrational and rotational temperatures of the ground state, respectively. $\langle\sigma_e v_e\rangle_{v'N'}^{vN}$ is the electron-impact excitation rate coefficient, which can be approximated [6] as $\langle\sigma_e v_e\rangle_{v'N'}^{vN} = \langle\sigma_v v_e\rangle_{v'N'}^{vN} a_{N'}^{N}$, where

$\langle\sigma_{\rm v}v_{\rm e}\rangle^{vN}_{v'N'}$ is the vibronic excitation rate coefficient, and $a^N_{N'}$ is the relative probability of the rotational transition. $\langle\sigma_{\rm v}v_{\rm e}\rangle^{vN}_{v'N'}$ is assumed to be equal to the Franck-Condon factor (FCF) multiplied by the rate coefficient

$$\langle\sigma_{\rm v}v_{\rm e}\rangle^{vN}_{v'N'} = q^{vN}_{v'N'}\int_{E_{\rm th}}^{\infty}\sigma_{\rm e}(E)v_{\rm e}f_{\rm e}(E)dE, \qquad (4)$$

where $q^{vN}_{v'N'} = |\langle\phi_{\rm v}|\phi'_{\rm v}\rangle|^2$ is the FCF, $E_{\rm th}$ is the threshold energy of the excitation, $\sigma_{\rm e}(E)$ is the electronic excitation cross section, and $f_{\rm e}(E)$ is the electron energy distribution function. It should be noted that the dependence on the internuclear distance is neglected in eq. (4) since the transition is optically forbidden. The probability $a^N_{N'}$ can be expressed both for the singlet-singlet [12] and singlet-triplet [13] transitions as

$$a^N_{N'} = \frac{1}{2}[1+(-1)^{N+N'}] \times \sum_r \bar{Q}_r(2N'+1)\begin{pmatrix} N' & r & N \\ 1 & -1 & 0\end{pmatrix}^2, \qquad (5)$$

where $\bar{Q}_r$ is the normalized partial cross section which satisfies a condition $\sum_r \bar{Q}_r = 1$. Dataset used for the above processes is summarized in [7].

3. Experiments

Experiments were carried out using a hollow-cathode discharge chamber at the University of Tokyo. Details of the setup are described elsewhere [14]. Briefly, the device consisted of a copper anode and an aluminum cathode. The cathode had face-to-face twin holes for diagnoses. In the present experiment, dc-glow discharges with discharge voltages of 219-247 V and discharge currents of 20-70 mA were sustained. The background gas pressure measured by a capacitance manometer was fixed to 77 Pa. The electron temperatures and densities measured by a double probe were 2.6-4.7 eV and 0.79-2.3 $\times$ 10^{16} $\rm m^{-3}$, respectively.

Emission from the plasma was collected using an objective lens with a spot size of approximately 10 mm in diameter at the center of the cathode. The collected emission was dispersed using a Czerny-Turner mounted spectrometer with a focal length of 1 m and 2400 grooves/mm holographic grating. The dispersed spectrum was detected using a photomultiplier tube (PMT) detector (Hamamatsu R928) operated at the temperature of -30 degree. The PMT consisted of a multi-alkali photo-cathode and UV glass envelope with the applicable wavelength range of 185-900 nm. The entrance and exit slit widths of the spectrometer were set to 80 μm corresponding to a wavelength resolution of $\Delta\lambda_{\rm FWHM} = 0.023$ nm. The sensitivity of the spectroscopic system including the window was absolutely calibrated using a tungsten halogen lamp.

4. Evaluation of the X-state ro-vibrational temperatures

Emission spectra were continuously recorded in the range of 380-660 nm, and the absolute wavelength was calibrated using the Balmer series. In this wavelength region, several H_2 bands were able to be observed, so that assignment was performed using Dieke's wavelength table [15]. After carefully excluding possibly contaminated lines, only the Q-branch ($\Delta N = N' - N'' = 0$) with $0 \le v' \le 3$ and $0 \le N' \le 5$ was used for the analysis. For the $I-B$ transition, the I-state population densities evaluated from ro-vibronic transitions which originate from the same upper ro-vibronic state were averaged.

The X-state ro-vibrational temperatures were measured by fitting eq. (2) to the experimentally obtained upper state populations. The most probable ro-vibrational temperatures were determined with discrete temperature steps of 10 K for $T_{\rm vib}$ and 1 K for $T_{\rm rot}$ so as to minimize χ^2. Here, $\chi^2 = [(n_{v'N'(\rm exp.)} - n_{v'N'(\rm cal.)})/\sigma_{n_{v'N'(\rm exp.)}}]^2$, where $n_{v'N'(\rm exp.)}$ and $n_{v'N'(\rm cal.)}$ are the upper state populations obtained from the experiment and calculation, respectively, and $\sigma_{n_{v'N'(\rm exp.)}}$ is the standard deviation of $n_{v'N'(\rm exp.)}$. Errors were estimated over a temperature range chosen such that $\Delta\bar{\chi}^2 = 1$, where $\bar{\chi}^2$ is the reduced χ^2.

Comparison of the ro-vibrational temperatures obtained from the d-a and I-B transitions is shown in Fig. 2. For the d-a transition, the vibronic population flow to the d-state has been analyzed based on a simple collisional-radiative

modeling [16, 17]. In the literature, they suggested that contributions of the cascade and electron impact excitation from the metastable $c^3\Pi_u$ state are significant. Even though, they concluded that because of the similarity in the adiabatic potential curve shapes among the triplet excited states as well as the excitation and deexcitation basically following the Franck-Condon principle, the relative vibronic population in the d-state can be evaluated under the coronal approximation without large error [17]. On the other hand, for the I-B transition, the above assumption may not be justified since singlet states have difference in their potential curve shapes. Significantly higher ro-vibrational temperatures measured from the I-B transition, therefore, may indicate the violation of the coronal approximation. Note that for the $I - B$ transition, slight decrease in the spontaneous emission coefficient with increasing v' and N' is reported [18]. When we consider this effect, the evaluated ro-vibrational temperatures become slightly higher.

5. Conclusion

Excitation-emission models based on the coronal approximation were developed for the H_2 $d^3\Pi_u$-$a^3\Sigma_g^+$ and $I^1\Pi_g$-$B^1\Sigma_u^+$ transitions. The $X^1\Sigma_g^+$ state ro-vibrational temperatures obtained from both the transitions were compared. The ro-vibrational temperatures evaluated from the I-B transition are significantly higher than those from the d-a transition. One of explanations for this deviation is the violation of the coronal approximation in evaluating the relative rovibronic population for the I-B transition.

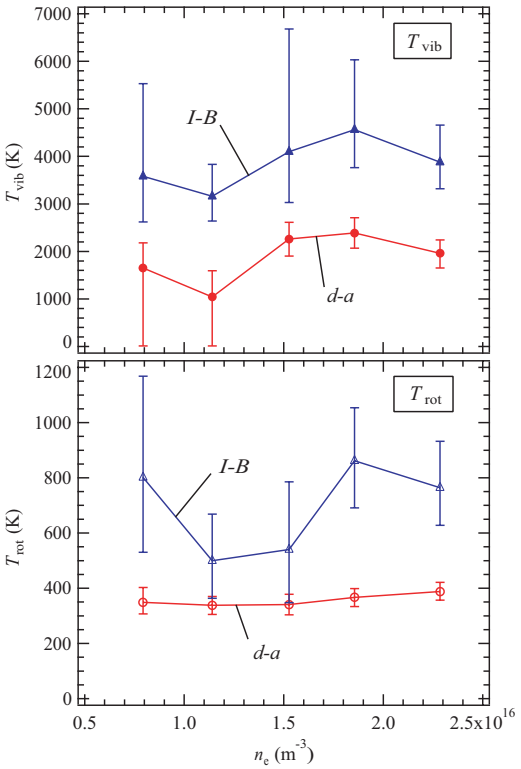

Figure 2. Ro-vibrational temperatures of the X-state evaluated from the d-a and I-B transitions as a function of n_e.

Acknowledgments

This work was partly supported by the Japan Atomic Energy Agency and National Institute for Fusion Science (NIFS08KOAP020).

REFERENCES

1. R. F. G. Meulenbroeks, R. A. H. Engeln, J. A. M. van der Mullen, and D. C. Schram, *Phys. Rev. E* **53**, 5207 (1996).
2. G. C. Stutzin, A. T. Young, H. F. Döbele, A. S. Schlachter, and K. N. Leung, *Rev. Sci. Instrum.* **61**, 619 (1989).
3. T. Mosbach, H-M. Katsch, and H. F. Döbele, *Phys. Rev. Lett.* **85**, 3420 (2000).
4. S. A. Astashkevich, M. Käning, E. Käning, N. V. Kokina, B. P. Lavrov, A. OHL, and J. Röpcke, *J. Quant. Spectrosc. Radiat. Transfer* **56**, 725 (1996).
5. U. Fantz and B. Heger, *Plasma Phys. Control. Fusion* **40**, 2023 (1998).
6. B. Xiao, S. Kado, S. Kajita, and D. Yamasaki, *Plasma Phys. Control. Fusion* **46**, 653 (2004).
7. T. Shikama and S. Kado, *J. Plasma Fusion Res. SERIES* **8**, 389 (2009).
8. M. L. Ginter, *J. Chem. Phys.* **46**, 3687

(1967).
9. U. Fantz, B. Schalk, and K. Behringer, *New J. Phys.* **2**, 7.1 (2000).
10. U. Fantz and D. Wünderlich, *At. Data Nucl. Data Tables* **92**, 853 (2006).
11. J. Tatum, *Astrophys. J. Suppl.* **14**, 21 (1967).
12. B. P. Lavorv, V. N. Ostrovsky, and V. I. Ustimov, *J. Phys. B* **14**, 4389 (1981).
13. D. K. Otorbaev, V. N. Ochkin, P. L. Rubin, S. Yu. Savinov, N. N. Sobolev, S. N. Tskhai, *Proc. Lebedev Phys. Inst.* **179 Suppl. 2**, 121 (1989).
14. D. Yamasaki, S. Kado, B. Xiao, Y. Iida, S. Kajita, and S. Tanaka, *J. Phys. Soc. Jpn.* **75**, 044501 (2006).
15. H. M. Crosswhite, "The hydrogen molecule wavelength tables of Gerhard Heinrich Dieke" *Wiley-Interscience* (1972).
16. P. T. Greenland, *Proc. R. Soc. Lond. A* **457**, 1821 (2001).
17. P. T. Greenland, *Contrib. Plasma Phys.* **42**, 608 (2002).
18. S. A. Astashkevich and B. P. Lavrov, *Opt. Spectrosc.* **89**, 13 (2000).